Integral-equation approach for the Bean critical-state model in demagnetizing and nonuniform-field geometries

K. L. Telschow and L. S. Koo
Idaho National Engineering Laboratory, EG&G Idaho Inc., Idaho Falls, Idaho 83415-2209
(Received 26 April 1994)

This paper describes an integral-equation approach to solving for the flux-front profile in the critical-state model. Both nonuniform external fields and demagnetizing geometries can be accommodated as long as cylindrical symmetry is preserved. The solution for a sphere in a uniform external field is presented and compared with those of other calculation techniques.

INTRODUCTION

The critical-state model was developed to account for flux pinning in superconductors.[1,2] This model assumes current flows in a type-II superconductor only at a local limiting or critical current value. Penetration of magnetic flux into the material is determined from the local critical current through Maxwell's relation. Flux first enters a solid object from the surface as an external field is applied. Initially, assuming zero-field cooling (ZFC), screening currents flowing at the critical current density (J_c) are established in the superconductor that shield the object's interior from magnetic-field penetration. These currents penetrate to a depth known as the flux-front boundary, where the magnetic flux density drops to zero. Within this boundary, total shielding takes place. As the external field is increased, the flux-front boundary penetrates deeper into the object until eventually the object is completely filled with screening currents. The value of the external field at this point is known as the full field-penetration value (H^*). Screening currents are assumed to flow only at the local critical current value, which depends on the material microstructure (pinning force) and the local field. The Bean[1] critical-state model assumes that J_c is independent of the local field; this is assumed throughout this paper, although extension of the approach to field-dependent critical currents is possible.

The primary use of the critical-state model is for determining the local critical current for a given sample. This is often accomplished by using the model to calculate the magnetization of a sample as it is brought through a magnetization cycle with an external field. This calculation is straightforward for sample geometries that do not exhibit demagnetization effects due to field lines crossing the sample surface. Therefore the sample geometries often assumed are cylinders or plates in fields parallel to the sample surfaces. Also, some sample shapes can be approximated by ellipsoidal shapes with known demagnetizing coefficients. The high-T_c superconducting materials are extreme type II and can be described by the critical-state model. Recent calculations of the expected magnetization as a function of the external field have been very successful.[3,4] These calculations are straightforward enough that even field-dependent local critical currents can be taken into account analytically.

The situation is much more complicated if the sample shape or field configuration involves demagnetizing effects. One such case, which often occurs in practice, is that of a disk or plate in a field perpendicular to the sample plane. This geometry is the extreme for demagnetization, but is often preferred experimentally. The full critical state (completely filled sample) in this geometry has been treated numerically and the results are used to predict the fields above the sample surface with good precision.[5-7] Partially filled samples, where the flux front has not penetrated completely, are more complicated; however, results have been published recently for which an optimization technique was used to determine the boundary where the magnetic field inside the sample is zero for a given external field.[8,9] This method appears to work well and has been extended to both spheres and ellipsoids of various shapes. However, this procedure has been questioned and it has been proposed that, in order to have a field-free region inside a solid object, the flux-penetration region cannot be filled with a single-value current, as assumed in the Bean model.[10]

This paper supports the idea that it is possible to find a field-free region, agrees with previous work done with this idea,[9] and presents an alternative approach for determination of the flux-front profile. An integral equation is developed for the external field derivative of the flux-front boundary. Successive applications of this equation can generate a new boundary from an old one, leading to determination of the boundary for any external field and prior history. The model is based on known solutions for the fields from a single current loop and is therefore restricted to cylindrically symmetric problems. The approach, method, and results for a sphere in an external uniform field are presented.

THEORETICAL APPROACH

Figure 1 shows a superconducting sphere placed in a uniform external magnetic field, $\mathbf{H}^{\text{ext}}=H_z^{\text{ext}}\hat{\mathbf{e}}_z$, where $\hat{\mathbf{e}}_z$ is the unit vector along the z axis. Cylindrical symmetry requires any induced current inside the sphere to travel along the azimuthal direction, $\hat{\mathbf{e}}_\phi=\hat{\mathbf{e}}_z\times\hat{\mathbf{e}}_r$, where $\hat{\mathbf{e}}_r$ is the unit vector in the radial direction. All induced currents

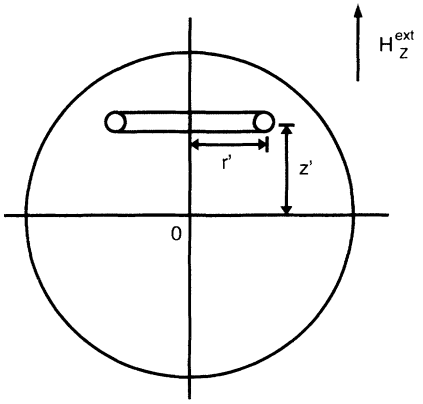

FIG. 1. A sphere in a uniform external field showing the horizontal current loops that make up the critical-state currents.

inside the sphere form loops in the x,y plane with radius and vertical coordinates (r',z') measured with respect to the center of the sphere. According to the Bean critical-state model, a region of shielding current is created, starting at the sphere boundary and extending inward, that satisfies $\nabla\times\mathbf{B}=\mu_0\mathbf{J}_C$. This leads to a decrease of the net magnetic flux density from the surface to zero at the flux-front boundary. The region inside this boundary is free of magnetic field, shielded completely by the induced screening currents. The goal of the model for this demagnetizing geometry is to predict the shape of this field-free region for calculation of magnetization and other measurable parameters for comparison with experimental results.

The approach described below uses the vector potential to determine where the flux-front boundary is located. The boundary, defined as the surface on which the total magnetic field is zero, can be described by a vector equation.[9] However, it can also be defined as a surface of zero vector potential, as shown below. The use of the vector potential simplifies the calculations since only one component is needed for problems of cylindrical symmetry.

Consider a simply connected region Ω with a closed surface $\partial\Omega$, with no currents inside Ω and only tangential currents on $\partial\Omega$. Let the normal component of the magnetic induction, B_n, be zero on $\partial\Omega$ (normal unit vector $\hat{\mathbf{e}}_n$ points into Ω), then, following Refs. 8 and 9, $\mathbf{B}=\mathbf{0}$ for all points in Ω and $\mathbf{A}=\mathbf{0}$ for cylindrically symmetric geometries, where $\mathbf{B}=\nabla\times\mathbf{A}$. This can be shown as follows. Given $\mathbf{J}=\mathbf{0}$ inside Ω, $\nabla\times\mathbf{B}=\mathbf{0}$, with $\mathbf{B}=\mu_0\mathbf{H}$ and $B_n=0$. Then, since $\nabla\cdot\mathbf{B}=0$, $\mathbf{B}=\nabla\Psi$ and $\nabla^2\Psi=0$, and the following integral becomes

$$\int_\Omega \nabla\cdot\Psi\nabla\Psi\, d\tau=\int_\Omega \Psi\nabla^2\Psi\, d\tau+\int_\Omega |\nabla\Psi|^2 d\tau=\int_\Omega B^2 d\tau\ . \tag{1}$$

By applying the divergence theorem, this integral becomes

$$\int_{\partial\Omega}\Psi\mathbf{B}\cdot d\mathbf{s}=\int_{\partial\Omega}\Psi B_n ds=\int_\Omega B^2 d\tau=0\ . \tag{2}$$

Since B^2 is positive definite, $\mathbf{B}=\mathbf{0}$ everywhere in Ω and on $\partial\Omega$. Consequently $\nabla\times\mathbf{A}=\mathbf{0}$ in Ω and, along with the Coulomb gauge $\nabla\cdot\mathbf{A}=0$, $\mathbf{A}=\nabla\Phi$, $\nabla^2\Phi=0$. Repeating the above argument for the vector potential yields

$$\int_{\partial\Omega}\Phi A_n ds=\int_\Omega A^2 d\tau=0\ . \tag{3}$$

For cylindrical symmetry, the component of the vector potential normal to the surface is always zero, and therefore $\mathbf{A}=\mathbf{0}$ inside Ω and on $\partial\Omega$.

The converse argument is also true: given $\mathbf{A}=\mathbf{0}$ inside Ω and on $\partial\Omega$, then it can be shown that $B_n=0$ on $\partial\Omega$ and, from the above, $\mathbf{B}=\mathbf{0}$ in Ω. The key to showing this result is that there is no magnetic flux penetrating through $\partial\Omega$. Consider an infinite plane intersecting Ω with the intersecting area being K, which has a normal vector pointing into Ω. This intersection forms a closed loop Σ_K (with a counterclockwise sense) on $\partial\Omega$. Then, using Stokes's theorem, the magnetic flux Π_K through Σ_K into Ω is

$$\Pi_K=\oint_{\Sigma_K}\mathbf{A}\cdot dl=\int_K \nabla\times\mathbf{A}\cdot d\mathbf{s}=\int_K B_n ds\ . \tag{4}$$

Since $\mathbf{A}=\mathbf{0}$ on $\partial\Omega$, $\Pi_K=0$. In the limit as the size of K is shrunk to zero, the above argument states that $B_n=0$ on $\partial\Omega$ and, by the previous argument, $\mathbf{B}=\mathbf{0}$ in Ω.

In the following sections, the flux-front surface is defined as that surface on which the vector potential is zero.

ZERO-FIELD-COOLED SPHERE FLUX-FRONT BOUNDARY

Let the radius of the sphere be r_0 and the magnitude of its critical current density be J_c. Throughout, it is assumed that the critical field for entrance of a single flux line (H_{c1}) is zero. In this case, flux begins to enter the sphere immediately as the external field is increased from zero. The vector potential produced by the external field is

$$A_\phi^{\text{ext}}(r,z)=\frac{\mu_0 H_z^{\text{ext}} r}{2}\ . \tag{5}$$

Inside the sphere, the induced field A_ϕ^{ind} is

$$A_\phi^{\text{ind}}(r,z)=-\int_{-r_0}^{r_0}dz'\int_{\rho(z',H_z^{\text{ext}})}^{\sqrt{r_0^2-z'^2}}dr'\mu_0 J_c a_\phi(r,z;r',z')\ , \tag{6}$$

where $\mu_0 a_\phi(r,z;r',z')$ is the vector potential at (r,z) due to a single current loop of unit current with radius and vertical position (r',z') and the minus sign indicates that the induced currents shield the external field. This function is well known[11] and can be written in terms of complete elliptic integrals of the first and second kind as

$$a_\phi(r,z;r',z')=\frac{1}{\pi}\left[\frac{r'}{r}\right]^{1/2}\left[\frac{(1-k^2/2)K(k^2)-E(k^2)}{k}\right]\ , \tag{7}$$

where

$$k^2=\frac{4rr'}{(r+r')^2+(z-z')^2}\ .$$

The flux-front surface is described by $r=\rho(z,\beta)$ where the external field dependence is included in the normalization parameter $\beta=H_z^{\rm ext}/r_0 J_c$. The total normalized vector potential at (r,z) is given by

$$A_\phi(R,Z,\beta)=\frac{A_\phi^{\rm ext}+A_\phi^{\rm ind}}{\mu_0 r_0^2 J_c}$$
$$=\frac{\beta R}{2}-\int_{-1}^{1}dZ'\int_{P(Z',\beta)}^{\sqrt{1-Z'^2}}dR'\times a_\phi(R,Z;R',Z') \quad (8)$$

where all lengths are normalized to the sphere radius $R=r/r_0$, $Z=z/r_0$, $P=\rho/r_0$, etc. The position of the flux-front surface is obtained by finding those positions $[P(Z,\beta),Z]$ where the vector potential of Eq. (8) is zero. This is a difficult problem in general, but can be simplified by reducing Eq. (8) to a single integral as follows. In general, $H_Z^{\rm ext}$, and therefore β, is a function of time. This paper deals only with the quasistationary states of the critical state. The time scale for changes in the external field is typically very much longer than that exhibited by flux-line motion, so the model always assumes a sequence of stationary states uniquely defined by the history and present value of the external field. Changes in the external field, therefore, produce a corresponding change in the flux-line profile position, but at all times the vector potential on this profile is zero. Therefore a requirement of the flux-penetration profile is that

$$A_\phi(P(Z,\beta+\Delta\beta),Z)=A_\phi(P(Z,\beta),Z)$$
$$=0$$
$$\Longrightarrow\frac{\partial A_\phi(P(Z,\beta),Z)}{\partial\beta}=0. \quad (9)$$

Another way of stating this requirement is that, if a coil is placed on this flux front, that is, with radius $P(Z,\beta)$, no flux passes through the coil. Differentiating Eq. (8) and evaluating on the flux-front boundary yields

$$\frac{P(Z,\beta)}{2}+\int_{-1}^{1}dZ'a_\phi(P(Z,\beta),Z;P(Z',\beta),Z')\frac{\partial P(Z',\beta)}{\partial\beta}=0\,. \quad (10)$$

This is a single-integral equation describing the flux-front surface.

NUMERICAL PROCEDURE FOR FLUX-FRONT RESOLUTION

In Eq. (10) both the flux-front profile and its rate of penetration (the derivative term) are unknown. As suggested by the critical-state model, when the external field β is initially turned on, flux enters the sphere from the surface. Thus $P(Z,\beta=0)=\sqrt{1-Z^2}$ and, when β is small, the flux-front profile is very near the sphere surface. With substitution of a known $P(Z,\beta)$, Eq. (10) becomes a so-called linear Fredholm integral equation of the first kind for the unknown derivative $\partial P/\partial\beta$. This type of linear integral equation is well understood and there are several algorithms for resolving it. Most of these algorithms use the iteration approach; convergence of the iteration is either guaranteed by rigorous mathematical arguments or shown to be so in applications where no mathematical proof is available. A simple convergent iteration scheme proposed and analyzed by Gold[12] was used to resolve Eq. (10) (see the Appendix). Using this iteration technique, the derivative term can be resolved satisfactorily within a finite number steps, typically two. For the case of a very small external field, the derivative term can be determined by equating the low-field flux penetration to a surface current density as outlined in Ref. 9, with the result $[\partial P(Z,\beta)/\partial\beta]|_{\beta=0}=-\frac{3}{2}$. This result is verified by substituting into Eq. (10) where satisfactory convergence is achieved with the first iteration. However, the initial value of the derivative quantity is not necessarily needed. When not available, it can be resolved from Eq. (10) by applying Gold's algorithm, given a reasonable trial function. As the external field is increased to $\beta=\Delta\beta$, the new flux-front profile is approximated by

$$P(Z,\beta=\Delta\beta)=P(Z,\beta=0)+\frac{\partial P(Z,\beta=0)}{\partial\beta}\Delta\beta\,.$$

This approximation is acceptable as long as the increment $\Delta\beta$ is sufficiently small. With this approximation, the flux-front profile at $\beta=\Delta\beta$ is known but its derivative is yet to be determined. This is the same situation as at the beginning when $\beta=0$. The above procedure is repeatedly employed, using the previous derivative term as a trial function, to solve for the new derivative term corresponding to each profile. The proposed methodology for resolving Eq. (10) involves an incremental numerical scheme with N steps $1\le n\le N$ and an iteration technique with M steps $1\le i\le M$. The complete method can be summarized by expressing Eq. (10) as

$$\frac{P_n}{2}+\int_{-1}^{1}dZ'a_\phi(P_n,Z;P_n',Z')\left[\frac{\partial P}{\partial\beta}\right]_{n,i}=0 \quad (11)$$

with $P_n=P(Z,\beta_n)$ and $(\partial P/\partial\beta)_{1,1}=-\frac{3}{2}$. The values for the flux-front boundary are given by $P_{n+1}=P_n+(\partial P/\partial\beta)_{n,M}\Delta\beta$.

Figure 2 shows several intermediate calculated flux-front surfaces as a function of the normalized radial distance R and vertical distance Z. Because of spherical symmetry, only the results in one quadrant are shown. The intersection point on the Z axis (Z_0) was determined for each new flux-front surface. From this intersection point to the origin, the same number of calculation points was used for each flux-front surface to obtain similar accuracy between fronts. The calculated profiles agree well with those given in Ref. 9.

The method of resolving Eq. (10) can be verified by comparing the full field-penetration value obtained with that determined analytically. Figure 3 shows the distance from the center of the sphere (R_0), determined numerically, of the flux-front surface. The value of β that fills the sphere with current loops and produces zero field at the center is called β^* and is calculated analytically by setting

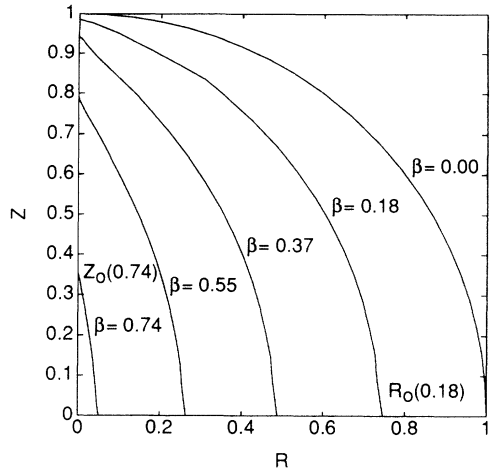

FIG. 2. Flux-front profiles calculated from Eq. (11) for the first quadrant of the sphere as a function of applied field.

$$\mu_0 r_0 H_Z(0,0)=\beta^*-\int_{-1}^{1}dZ'\int_0^{\sqrt{1-Z'^2}}dR'h_Z(0,0;R',Z')$$
$$=0\ ,\quad \beta^*=\frac{\pi}{4}\ , \tag{12}$$

where

$$h_Z(0,0;R',Z')=\frac{1}{2}\frac{R'^2}{(Z'^2+R'^2)^{3/2}}\ .$$

Numerically, $\beta^*=0.789$ at $R_0=0$. The numerical and analytical values agree to within 0.5%, consistent with the expected accuracy of the calculation procedure used.

MAGNETIC MOMENT CALCULATION

Once the flux-front profile's dependence on the external field for the ZFC case is known, then the response of the sample to a complete cycle of changes in the external field can be readily calculated. The following illustrates this by calculating the magnetization hysteresis curve for the sphere. The magnetic moment of the current distribution in the sphere is $\mathbf{m}=m\hat{\mathbf{e}}_Z$, where $\mathbf{m}=\frac{1}{2}\int \mathbf{r}\times J_c d\tau$, and the integral is taken over the filled portion of the sphere.

This becomes

$$m(\beta)=-\int_{-r_0}^{r_0}dz'\int_{\rho(z',\beta)}^{\sqrt{r_0^2-z'^2}}dr'\pi r'^2 J_c\ ,$$
$$m(\beta^*)=-\frac{\pi^2 J_c r_0^4}{8}\ . \tag{13}$$

The magnetization of the sphere in normalized coordinates is then

$$M(\beta)=\frac{m(\beta)}{(\frac{4}{3}\pi r_0^3)}$$
$$=-\left[\frac{3J_c r_0}{4}\right]\int_{-1}^{1}dZ'\int_{P(Z',\beta)}^{\sqrt{1-Z'^2}}dR'R'^2$$
$$=M^*\left[-1+\frac{8}{3\pi}\int_{-1}^{1}dZ'P^3(Z',\beta)\right]\ , \tag{14}$$

where $M^*=M(\beta^*)=3\pi J_c r_0/32$.

MAGNETIZATION HYSTERESIS LOOP

The foregoing describes the magnetization as the external field is increased from the ZFC state to some value $\beta_{\max}<\beta^*$. When the external field is subsequently reduced to β from $\beta_{\max}$, a second flux-front boundary enters the sphere from the outer surface with currents flowing at $+J_c\hat{\mathbf{e}}_\phi$. It is now necessary to label the two flux fronts as $P_1(Z,\beta_{\max})$ and $P_2(Z,\beta)$. The first front is filled with negative currents (defined as flowing in the direction that produces a magnetic moment that opposes the external field) and remains fixed as the second front fills with positive currents, as depicted in Fig. 4. Now the total normalized vector potential [normalization factor given in Eq. (8)] at an arbitrary location (R,Z) is

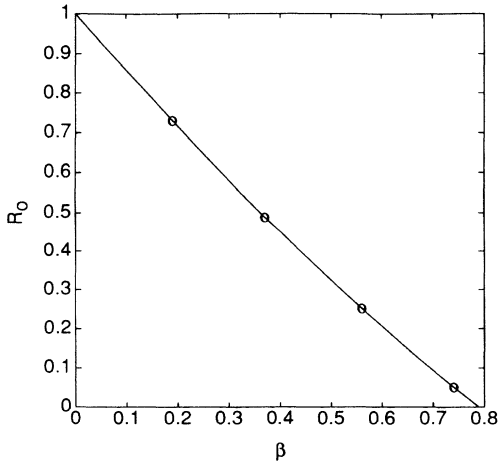

FIG. 3. Locations of the flux-front profile intersection R_0 with the sphere axis as a function of the applied field.

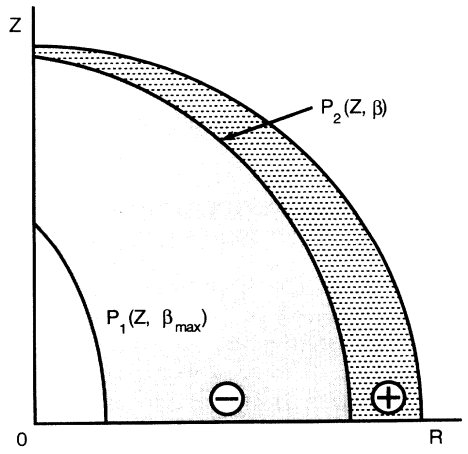

FIG. 4. Schematic of the fixed initial flux-front profile (P_1) and the second profile (P_2) entering as the field is reduced from its maximum value.

$$A_2(R,Z,\beta)=\frac{\beta R}{2}-\int_{-1}^{1}dZ'\int_{P_1(Z',\beta_{\max})}^{\sqrt{1-Z'^2}}dR'a_\phi(R,Z;R',Z')+2\int_{-1}^{1}dZ'\int_{P_2(Z',(\beta_{\max}-\beta))}^{\sqrt{1-Z'^2}}dR'a_\phi(R,Z;R',Z') . \quad (15)$$

The factor of 2 in the last integral is introduced to account for the negative current neutralizing the previous positive current and then filling that space. Let $\beta'=\beta_{\max}-\beta$; then application of the previous argument maintaining the total vector potential zero on the first flux-front boundary by introducing a second boundary similarly to the first yields

$$\frac{P_2(Z,\beta')}{2}+2\int_{-1}^{1}dZ'a_\phi(P_2(Z,\beta'),Z;P_2(Z',\beta'),Z')\times\left[\frac{\partial P_2(Z',\beta')}{\partial\beta'}\right]=0 . \quad (16)$$

This is the flux-front equation for P_2. The equation for the ZFC flux front P_1 is recovered if $\beta'=2\beta''$. Therefore

$$P_2(Z,\beta)=P_1\left[Z,\frac{\beta_{\max}-\beta}{2}\right],\quad 0<\beta_{\max}-\beta<2\beta_{\max} ,$$

which retraces all the locations of P_1 but at a slower pace with respect to β. This accounts for the hysteresis observed in the critical-state model.

The total magnetic moment of the sphere for $\beta^*\geq\beta_{\max}>\beta>-\beta_{\max}$ is

$$M_2(\beta)=-\left[\frac{3J_c r_0}{4}\right]\left[\int_{-1}^{1}dZ'\int_{P_1(Z',\beta_{\max})}^{P_2(Z',\beta)}dR'R'^2-\int_{-1}^{1}dZ'\int_{P_2(Z',\beta)}^{\sqrt{1-Z'^2}}dR'R'^2\right] . \quad (17)$$

This can be written as

$$\frac{M_2(\beta)}{M^*}=+1+\frac{8}{3\pi}\int_{-1}^{1}dZ'P_1^3(Z',\beta_{\max})-\frac{16}{3\pi}\int_{-1}^{1}dZ'P_2^3(Z',\beta) , \quad (18)$$

or as

$$\frac{M_2(\beta)}{M^*}=\frac{M_1(\beta_{\max})}{M^*}-2\frac{M_1((\beta_{\max}-\beta)/2)}{M^*} . \quad (19)$$

A complete hysteresis curve for the magnetization is obtained by calculating P_3 for $-\beta_{\max}\rightarrow\beta\rightarrow\beta_{\max}$. The third flux-front profile, obtained in a similar manner to the second flux front, is given by $P_3(\beta)=P_1((\beta_{\max}+\beta)/2)$ for $-\beta_{\max}\rightarrow\beta\rightarrow+\beta_{\max}$ and the magnetization becomes

$$\frac{M_3(\beta)}{M^*}=-\frac{M_1(\beta_{\max})}{M^*}+2\frac{M_1((\beta_{\max}+\beta)/2)}{M^*} . \quad (20)$$

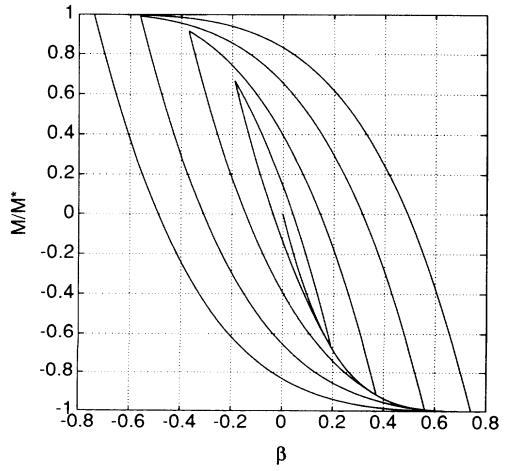

FIG. 5. Magnetization hysteresis loops for the sphere for various limiting fields up to the full penetration value β^*.

Figure 5 shows the resultant hysteresis curves for various values of the maximum external field $\beta_{\max}\leq\beta^*$. Once the magnetization curve is known, the response of the sphere to any time-dependent external field can be calculated. In particular, if the response to a sinusoidal field is found, then it can be decomposed and the sphere's harmonic response to ac fields is known.

CONCLUSION

A procedure has been presented for calculating the flux-front profile for a sphere in a uniform external field. The technique relies on finding a surface with zero vector potential for cylindrically symmetric problems. This surface is determined by simple integration of its derivative with respect to the external field, found by resolving a linear Fredholm integral equation of the first kind. It has been shown that the entire hysteresis loop response can be found by extension of the ZFC magnetization response with increasing external field. Other experimentally measured quantities relating to the critical state can be calculated directly from the hysteresis loop if the time dependence of the external field is known.

The technique developed in this paper for solving the critical-state model in the Bean approximation can be extended to field-dependent critical currents, other cylindrically symmetric sample shapes, and planar samples in cylindrically symmetric external fields.[13,14] This work is presently in progress.

ACKNOWLEDGMENTS

This work was supported by the U.S. Department of Energy, Office of Basic Energy Sciences, under DOE Idaho Operations Office Contract No. DE-AC07-76ID01570.

APPENDIX

In this section, the procedure used for resolving Eq. (10) with a known flux-front profile $P(Z,\beta)$ is given. To simplify the discussion, Eq. (10) is rewritten symbolically as

$$Kf=b\ , \tag{A1}$$

where f is the unknown vector $\partial P(Z',\beta)/\partial\beta$ and b is the given vector $-P(Z,\beta)/2$. The symbol K represents the integral operator with $a_\phi(P(Z,\beta),Z;P(Z',\beta),Z')$ being the kernel. Following the iterative resolution technique discussed by Gold,[12] the resultant quantity f can be expressed as the product of a diagonal matrix D and the known vector b as $f=Db$. In the first iteration, f is replaced by a guessed value $f^{(1)}$ and the corresponding output vector $b^{(1)}$ is then obtained by substituting $f^{(1)}$ into (A1). From this step, the matrix D has the first iterated value $D^{(1)}$ with its ith element being $D_{ii}^{(1)}=f_i^{(1)}/b_i^{(1)}$. For the next iteration step, the initial guess is $f^{(2)}=D^{(1)}b$. Then the above steps are repeated until the difference $|f^{(k)}-f^{(k-1)}|$ remains within an acceptable small value. The final vector $f^{(k)}$ is subsequently considered as the resolved value of f for the corresponding external field β. For all the results reported in this paper, $k=3$. At $\beta=0$ and with $f^{(1)}$ being the analytically exact value, $|f^{(k)}-f^{(k-1)}|$ remains acceptably close to zero for $k\geq 2$. However, knowledge of the analytically exact value for $f^{(1)}$ is not necessary. When other reasonable values are used instead, a satisfactory result can be achieved within a finite number of steps, often $k\leq 6$. At the full field-penetration value $\beta=\beta^*$, this iteration technique together with the incremental procedure mentioned in the main text returns a numerically estimated β^* within a 0.5% difference from the analytical value. Hence the validity of this iterative technique is verified at both $\beta=0$ and $\beta=\beta^*$.

[1]C. P. Bean, Phys. Rev. Lett. **8**, 250 (1962); Rev. Mod. Phys. **36**, 31 (1964).

[2]A. M. Campbell and J. E. Evetts, *Critical Currents in Superconductors* (Taylor & Francis, London, 1972).

[3]L. Ji, R. H. Sohn, G. C. Spalding, C. J. Lobb, and M. Tinkham, Phys. Rev. B **40**, 10 936 (1989).

[4]T. Ishida and R. B. Goldfarb, Phys. Rev. B **41**, 8937 (1989).

[5]D. J. Frankel, J. Appl. Phys. **50**, 5402 (1979).

[6]M. Däumling and D. C. Larbalestier, Phys. Rev. B **40**, 9350 (1989).

[7]L. W. Conner and A. P. Malozemoff, Phys. Rev. B **43**, 402 (1991).

[8]M. Ashkin, J. Appl. Phys. **50**, 7060 (1979).

[9]R. Navarro and L. J. Campbell, Phys. Rev. B **44**, 10 146 (1991); see also Phys. Rev. B **46**, 14 927 (1992); P. Chaddah and K. V. Bhagwat, Phys. Rev. B **46**, 14 926 (1992).

[10]K. V. Bhagwat and P. Chaddah, J. Phys. **33**, 521 (1989); see also Phys. Rev. B **46**, 14 926 (1992); R. Navaro and L. J. Campbell, Phys. Rev. B **46**, 14 927 (1992).

[11]W. R. Smythe, *Static and Dynamic Electricity*, 2nd ed. (McGraw-Hill, New York, 1950), pp. 270–271.

[12]R. Gold, Argonne National Laboratory Report No. ANL-6984, 1964 (unpublished).

[13]K. L. Telschow and T. K. O'Brien, Appl. Phys. Lett. **59**, 730 (1991).

[14]L. S. Koo and K. L. Telschow, *Review of Progress in Quantitative NDE*, edited by D. O. Thompson and D. E. Chimenti (Plenum, New York, 1994), Vol. 13B, pp. 1677–1681.

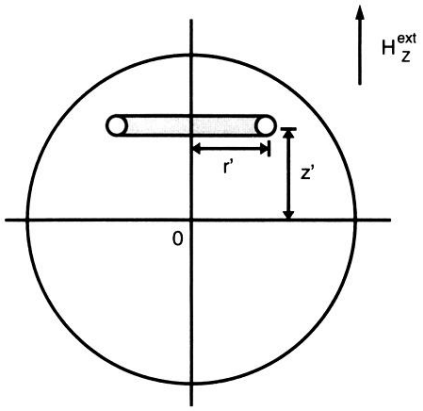

FIG. 1. A sphere in a uniform external field showing the horizontal current loops that make up the critical-state currents.

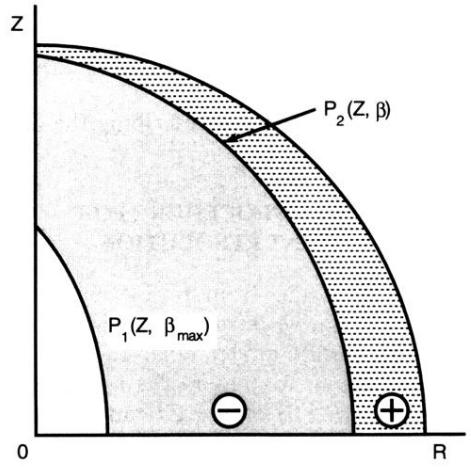

FIG. 4. Schematic of the fixed initial flux-front profile (P_1) and the second profile (P_2) entering as the field is reduced from its maximum value.